encit 2020

ABCM
Associação Brasileira de Engenharia e Ciências Mecânicas

18th Brazilian Congress of Thermal Sciences and Engineering
November 16-20, 2020 (Online)

ENC-2020-0436
NUMERICAL EVALUATION OF STATISTICALLY DEVELOPED HORIZONTAL SLUG FLOWS FROM THREE-DIMENSIONAL FIELDS

Pedro Roberto Barbosa Rocha
Angela Ourivio Nieckele
Department of Mechanical Engineering, Catholic University of Rio de Janeiro, PUC-Rio, 22451-900, Rio de Janeiro, RJ, Brazil
prbarbosr@gmail.com, nieckele@puc-rio.br

Abstract. *In this work, the dynamical behavior of an air-water slug unit cell over time was investigated. For that, three-dimensional numerical simulations were carried out in OpenFOAM. They included the Volume of Fluid (VOF) multiphase model and the κ-w Shear Stress Transport (SST) turbulence model. Slug parameters, such as the mean length, translational velocity and frequency were determined. A good correspondence between the results achieved here and those gathered from literature was found. From the 3D velocity field, wall shear stresses and momentum flux parameters were assessed. These results may be further used to improve correlations applied in one-dimensional models.*

Keywords: *slug flow, wall shear stress, momentum flux parameter, VOF*

1. INTRODUCTION

Gas-liquid horizontal intermittent flows are commonly found in the industry, such as in chemical plants and in the transportation of oil and gas. Such type of flow can cause different problems along a pipeline installation, like flow induce vibrations. It can also enhance corrosion (Thaker and Banerjee, 2016). In order to design successfully pipeline systems and related equipment, it is fundamental to study and predict the hydrodynamic behavior of these flows. The slug flow pattern, exhibited in Fig. 1, presents an alternation between a region fully occupied by liquid (blue) and another one composed by a liquid film under a gas bubble (red).

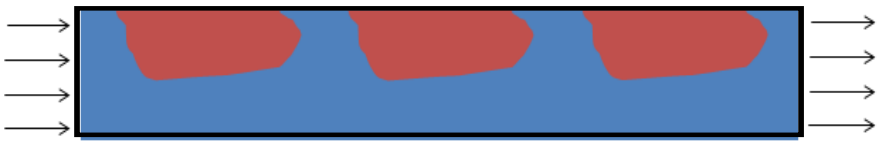

Figure 1. Slug flow pattern

Due to the complexity of the flow, several numerical simulations with different levels of approximation (1D or 3D) and modeling (Two-phase flow or VOF) have been performed (Simões et al, 2014; Pineda-Pérez et al. 2018). While Two-phase flow models treat the gas and the liquid separately, VOF simulations consider the whole domain is filled by a single phase with different properties. Regarding the experiments, capacitance sensors and image processing techniques are frequently employed to evaluate slug parameters (Fernandes et al., 2018).

One-dimensional models are especially attractive for the industry when very long pipelines are considered, due to the low demand of memory and computing resources. However, 1D models require several closure relations to deal with the momentum transfer between the wall and phases and across the gas-liquid interface, as well as the phase distribution along the cross-section. On the other hand, 3D simulations provide detailed volume fraction and velocity fields, but with high computing demand. Often, the closure relations are experimentally determined. An alternative methodology consists of determining the associated wall shear stresses and velocity distribution along a cross-section from a detailed 3D solution.

In order to handle the cyclic nature of slug flows, the slug unit cell concept (Taitel and Barnea, 1990), depicted in Fig. 2, was created. This approach considers the slug as statistically developed, i.e. its time-averaged physical quantities, such as the liquid holdup, do not change over time. In Fig. 2, l_b is the bubble length, l_s is the slug length, l_u is the unit cell length, u_{sg} is the superficial gas velocity, u_{sl} is the superficial liquid velocity and U_t is the slug translational velocity. The main objective of the present work is to evaluate statistically developed slug unit cells by the lens of a 3D Computational Fluid Dynamics (CFD) simulation within the software OpenFOAM. The results are compared against literature. Wall shear stresses and flux parameters at gas and liquid regions are computed along the unit cell. It represents a novelty that may lead to a new perspective of assessing friction factors for 1D models.

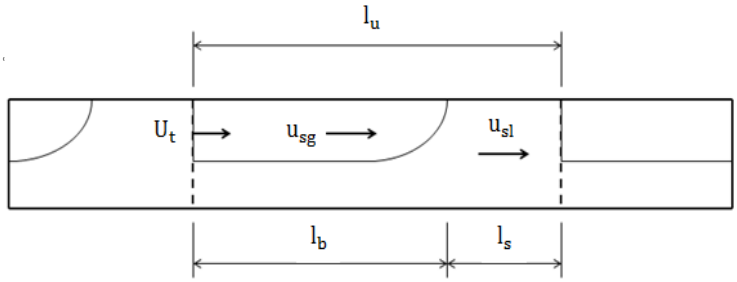

Figure 2. Unit cell concept

2. MATHEMATICAL AND NUMERICAL MODELING

The dynamics of one slug unit cell (see Fig. 2) was simulated through three-dimensional CFD techniques, employing the VOF technique. To do so, some hypotheses were assumed: air and water are the only working fluids and they have constant properties; the flow is incompressible and isothermal and the tube is horizontal and has no porosity. Since no heat exchange occurs in the present modeling, the energy conservation equation was not taken into account.

The unit cell was modeled employing a period boundary condition, i.e., a constant axial average pressure gradient (dp_m/dz) was imposed, where pressure is $P = p_m + p$, and all inlet quantities were equated to the outlet. The continuity and momentum equations are

$$\frac{\partial u_j}{\partial x_j} = 0 \tag{1}$$

$$\frac{\partial u_j}{\partial x_j} = 0 \quad ; \quad \frac{\partial}{\partial t}(\rho u_j) + \frac{\partial}{\partial x_j}(\rho u_j u_i) = -\frac{\partial P}{\partial x_i} + \rho g_i + \frac{\partial}{\partial x_j}\left(\mu_{ef}\frac{\partial u_i}{\partial x_j}\right) + f_{\sigma_i} \tag{2}$$

where ρ is the fluid density, u_j is the velocity component and g_i is gravity component. μ_{ef} is the effective turbulent viscosity to model the turbulence of the flow. A source term is employed in the momentum equation by the VOF method, only at the interface, to handle the interface curvature, $\vec{f}_\sigma = \sigma K \vec{n}\delta(n)$, where σ is the superficial stress, K is the interface curvature and $\vec{n}$ is the unit normal vector. This force was modeled according to Brackbill et al. (1992) as a continuum surface force (CSF).

To handle the turbulence, the governing equations selected to solve the problem were those of the SST-2003 k-ω turbulence model developed by Menter et al. (2003). This model was chosen because it combines the k-ε and k-ω turbulence models, ensuring the positive aspects of both, and it is also suitable to the treatment of flows with a relatively low Reynolds Number. In the SST-2003 k-ω turbulence model, the standard k-ε or the Wilcox k-ω model is activated according to the distance to the wall. The first one works better in the free stream region, and it is there where it is applied, while the second one predicts with more accuracy the flow in the viscous sublayer. A blending function is responsible for this switch between the models. The SST model is based on Reynolds Averaged Navier-Stokes (RANS) equations. A fluctuating contribution to the acceleration terms of the momentum conservation equations, also known as the Reynolds stress, arises as a result of the application of the Reynolds decomposition technique. As a matter of fact, the Reynolds stress is quite challenging to be handled. Regarding the SST model, this problem is addressed by assuming a linear constitutive relationship with the mean flow straining field, the Boussinesq hypothesis, and by evoking two additional equations, Eqs. (3) and (4). One equation for k, the turbulence kinetic energy, and another for ω, its specific rate of dissipation. Both quantities are then used to evaluate the turbulent eddy viscosity.

$$\frac{\partial}{\partial t}(\rho k) + \frac{\partial}{\partial x_i}(\rho k u_i) = \frac{\partial}{\partial x_j}\left(\Gamma_k \frac{\partial k}{\partial x_j}\right) + \tilde{G}_k - Y_k + S_k \tag{3}$$

$$\frac{\partial}{\partial t}(\rho \omega) + \frac{\partial}{\partial x_i}(\rho \omega u_i) = \frac{\partial}{\partial x_j}\left(\Gamma_\omega \frac{\partial \omega}{\partial x_j}\right) + G_\omega - Y_\omega + D_\omega + S_\omega \tag{4}$$

In Eqs. (3) and (4), S_k and S_ω are user-defined source terms, which were zero in the present modeling. Besides, Γ_k and Γ_ω represent effective diffusivities, while $\tilde{G}_k$ and G_ω are the production terms. Y_k and Y_ω stand for the dissipation of k and ω. Finally, D_ω represents the cross-diffusion modification, being also responsible for blending k-ε and k-ω models. The equations associated to each one of these terms were scrutinized by Menter et al. (2003). Although some model constants are required for solving these equations, for the sake of brevity, they will not be presented here. Their values are the same as those recommended by these authors. The turbulent eddy viscosity μ_t is defined by Eq. (5), where S is the modulus of the mean strain rate tensor, F_2 is a blending function and a_1 is a model constant.

$$\mu_t = \frac{\rho a_1 k}{max(a_1\omega, SF_2)} \tag{5}$$

In order to track the gas-liquid interface in space and time, the VOF method employs a marker function through a fixed grid. This marker function α indicates the volume fraction of a reference phase at each cell. It varies between 0 and 1. At a cell fully occupied by the reference phase, $\alpha = 1$, while where this phase is not present, $\alpha = 0$. At the interface cells, $0 < \alpha < 1$. Indeed, VOF guarantees a good mass conservation, has a simpler numerical implementation than other methods and is able to handle topologically complex interfaces. These positive aspects contributed for the VOF to be chosen in the present work. An important feature of the method is that the transport equation for α, Eq. (6), has to be solved so that the location of the interface at each time instant may be found. Moreover, fluid properties, such as density and viscosity, are function of the volume fraction α at each cell, as shown in Eqs. (7) and (8). In the equations below, μ_{ef} is the effective viscosity and subscripts 1 and 2 indicate fluids 1 and 2. Here, fluid 1 is liquid and fluid 2 is gas. The time discretization was handled with the first order Euler implicit scheme, while the Upwind scheme was used for the spatial discretization of the momentum equations. However, since the volume fraction equation is purely convective, care must be taken to minimize its diffusion. Thus, a 2nd order spatial discretization scheme was employed in the transport equation for the volume fraction field.

$$\frac{\partial \alpha}{\partial t} + \frac{\partial (\alpha u_j)}{\partial x_j} = 0 \tag{6}$$

$$\rho = \alpha\rho_1 + (1-\alpha)\rho_2 \tag{7}$$

$$\mu_{ef} = \alpha\mu_{ef,1} + (1-\alpha)\mu_{ef,2} \tag{8}$$

Appropriate geometry and mesh were designed to reproduce a slug unit cell. The domain length was defined by the sum of the mean slug length with the mean bubble length - Fig. 2. Due to the pipe symmetry, only half cylinder was considered, as shown in Fig. 3. The value for the pipe diameter was extracted from experiments (Nieckele et al., 2013), as well as mean bubble and slug lengths. For the case presented here, the pipe has 24 mm diameter and the computational domain has 3 m length, which is the size of one slug unit cell. The designed mesh has important features, such as the absence of deformed elements and refinement near the wall, to improve its quality. A grid test was conducted to attest the temporal and spatial convergence of the solution. By doubling the number of elements, slug length and translational velocity changed less than 5%. The maximum Courant Number was 1.0 and the entire 3D mesh has 405,600 elements. The boundary conditions are depicted in Fig. 3, which shows an illustrative bubble. A cyclic boundary condition with a prescribed pressure jump that drives the flow was imposed at its inlet and outlet planes. The no-slip boundary condition was applied at the pipe wall. At the symmetry plane, the symmetry boundary condition was employed.

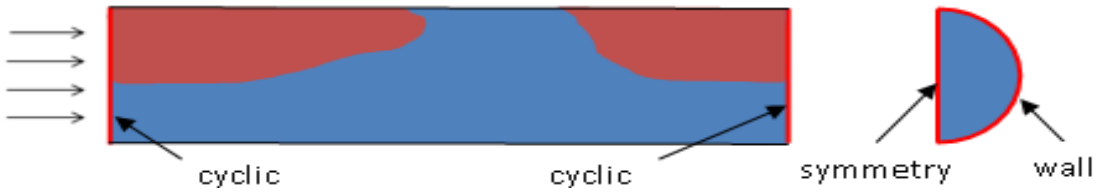

Figure 3. Boundary conditions

3. RESULTS AND DISCUSSION

In this section, the behavior of an air-water slug unit cell is studied over time. Main slug parameters (i.e. slug length, translational velocity and frequency) and wall shear stresses are evaluated. The superficial gas and liquid velocities of the selected case are equal to 0.8 and 0.3 m/s, respectively, which implies both phases are in the turbulent regime. A pressure gradient of 203 Pa/m, initially based on Lockhart and Martinelli (1949) correlation, is imposed, aiming to attain the desired superficial velocities. The total time-averaged liquid holdup is 0.38.

Before analyzing the results, it is of paramount importance to evaluate the temporal evolution of the flow in order to guarantee that a statistically steady state regime has been attained. Figure 4 illustrates the temporal evolution of the liquid holdup, α_L, and of the superficial gas and liquid velocities ($U_{sg} = Q_g/A; U_{sl} = Q_l/A$, where Q_k is the phase k volumetric flow rate, $k \in \{g, l\}$, and A is the pipe cross-section). The flow gets statistically developed after 2.5s of simulation, from when time-averaged liquid holdup and superficial velocities, evaluated at z = 1.5m, converge to a certain value along time. This fact is also shown in Fig. 4. The continuous lines represent the instantaneous values for the physical quantities, while the dashed ones are the time-averaged values.

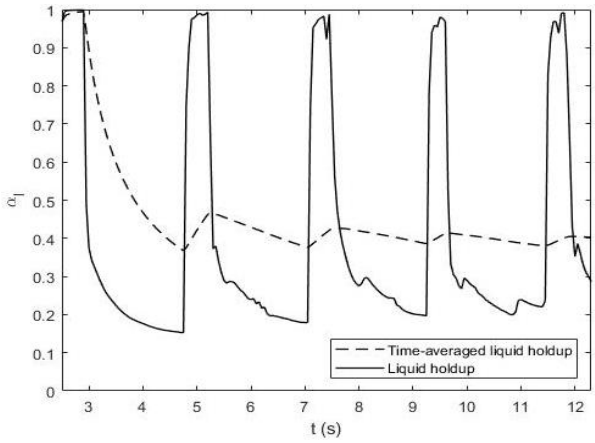

(a) liquid holdup

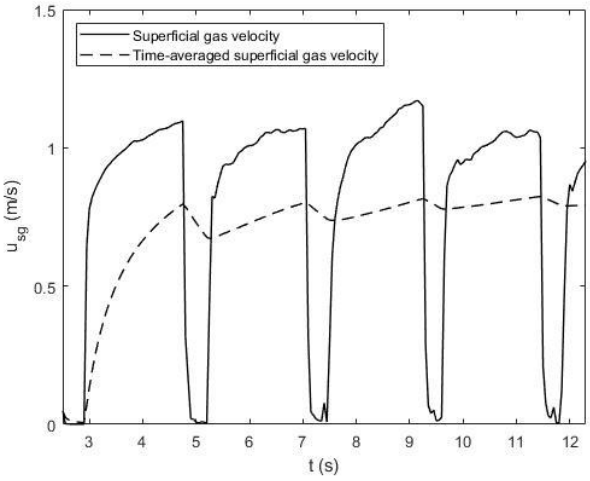

(b) superficial gas velocity

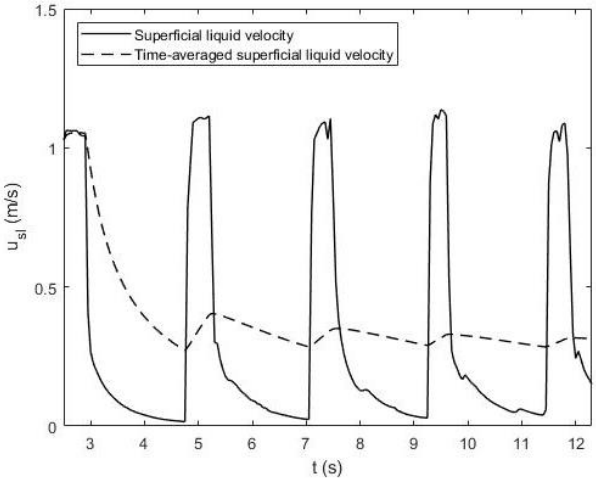

(c) superficial liquid velocity

Figure 4. Temporal evolution at z = 1.5m of the (a) liquid holdup, (b) superficial gas velocity and (c) superficial liquid velocity

In order to further validate the present methodology, slug flow parameters were evaluated and compared against literature. The mean slug length, normalized by the pipe diameter *D*, is shown in Tab. 1. This value is close to the reported by Nieckele *et al*. (2013), with a discrepancy of 8.5%. The slug translational velocity presented an excellent agreement. On the other hand, the slug frequency presented a larger discrepancy, of about 20%, which is still quite acceptable due to the larger uncertainties related to the measurement of this quantity.

Table 1. Slug flow parameters obtained from the 3D simulation and from Nieckele *et al*. (2013)

Parameters	$\overline{U_t}$ (m/s)	$\overline{l_s}/D$	Ω_s(1/s)
3D simulation	1.33	21.6	0.45
Nieckele *et al*. (2013)	1.33	19.9	0.56

The volume fraction field for different planes, in t = 11.75s, is depicted in Fig. 5. Figure 5(a) exhibits the phases at x = 0 (symmetry plane), while Figs. 5(b-d) show cross-sectional planes. The plane z = 1.2m, represented in Fig. 5(b), is in the stratified region of the flow, where there is a clear separation of gas and liquid phases. On the other hand, the plane z = 1.3m – Fig. 5(c) - is at the bubble nose. In this region, there is a thin liquid layer at the sides of the pipe, showing the faster-moving bubble tries to penetrate into the slug body. Finally, the plane z = 1.45m, from Fig. 5(d), is at the middle of the slug body, where the liquid almost fully occupies the pipe cross section. It is possible to notice the presence of a small gas bubble at the top of the pipe, which is recurrent in slug flows.

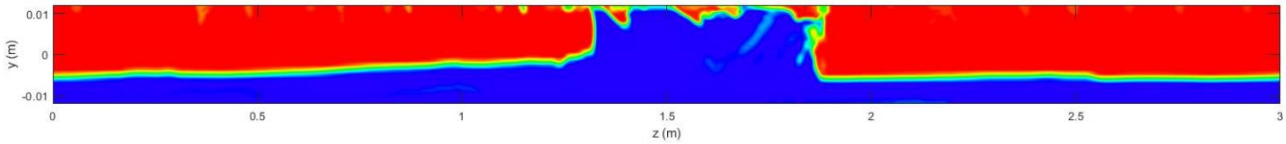

(a) x=0

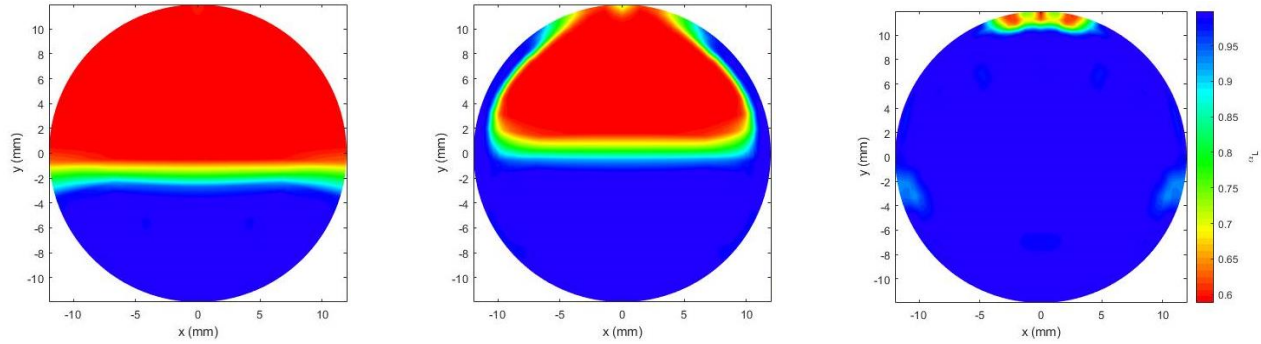

(b) z=1.2 m (c) z=1.3 m (d) z=1.45 m

Figure 5. Volume fraction field at (a) the symmetry plane, i.e. x = 0, (b) z = 1.2 m, (c) z = 1.3 m and (d) z = 1.45 m

Figure 6 show the perimeter-averaged gas and liquid wall shear stresses along the length of the computational domain in t = 11.75s. Note that the gas wall shear stress is almost constant in the bubble region (Fig. 6a) although the void fraction ($\alpha_G = 1 - \alpha_L$) and the superficial gas velocity u_{sg} vary along its length (Fig. 4). On the other hand, the liquid wall shear stress (Fig. 6b) presents a variation along the bubble, increasing from tail to nose, with a significant increase in the bubble nose region. However, it is approximately constant in the plug region, although there is an oscillation of its values due to the presence of small bubbles at the top of the liquid layer (Fig. 5d).

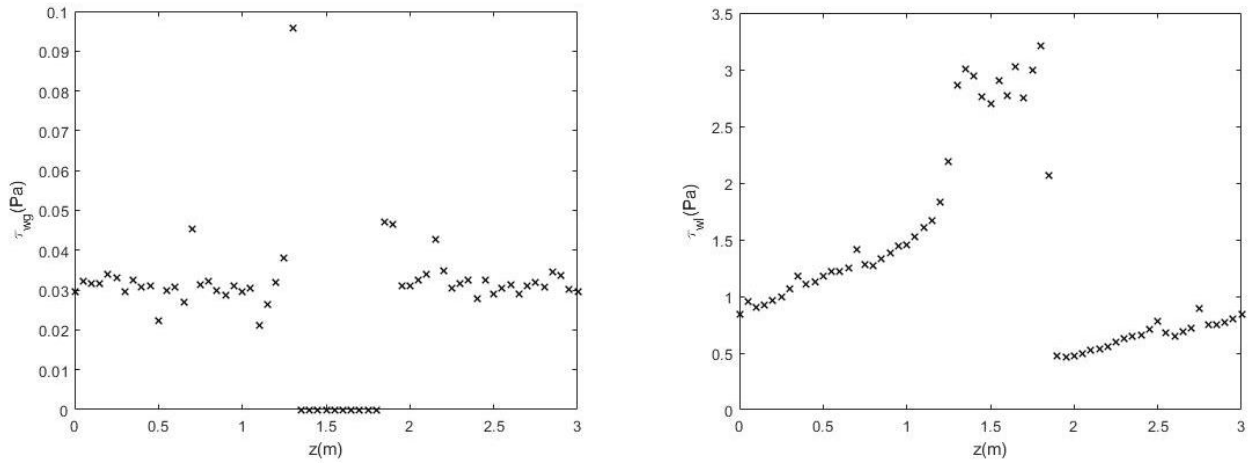

(a) gas phase (b) liquid phase

Figure 6. Axial variation of the perimeter-averaged wall shear stress of the (a) gas phase and (b) liquid phase.

The momentum flux parameter is a measure of the non-uniformity of the velocity profile in the momentum flux. It is defined by the following ratio:

$$C_k = \frac{\int_{A_k} u_k \, u_k \, d \, A_k}{\left[\left(\int_{A_k} u_k \, d \, A_k\right)\left(\int_{A_k} u_k \, d \, A_k\right)\right]} \tag{9}$$

Figure 7 shows that the gas momentum flux parameter is almost constant and equal to 1.2. The liquid momentum flux parameter at the bubble region is much smaller, approximately equal to 1.02, with a significant increase at the slug region, reaching the value of 1.17.

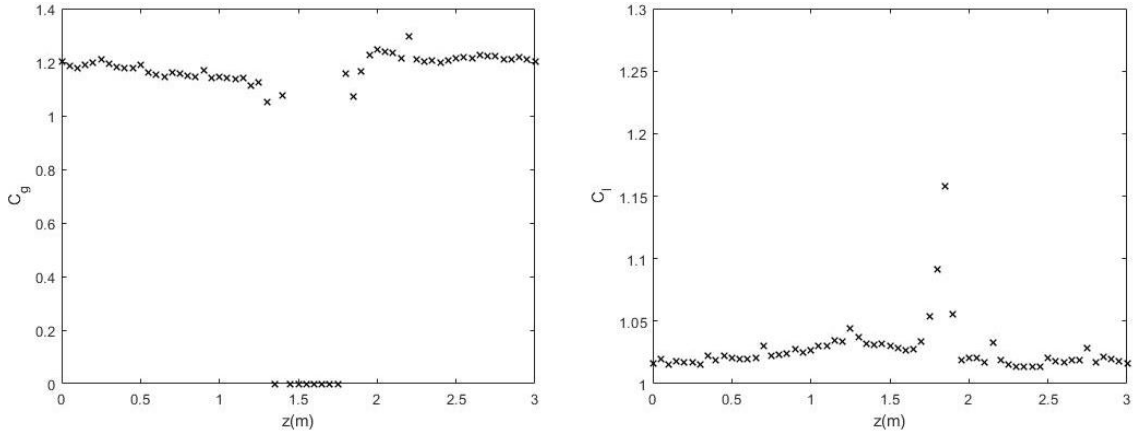

(a) gas phase (b) liquid phase

Figure 7. Momentum flux parameter of the (a) gas phase and (b) liquid phase

4. CONCLUSION

The dynamics of a statistically developed air-water slug unit cell was successfully reproduced in the present work by means of 3D numerical simulations involving the k-ω Shear Stress Transport (SST) turbulence model and the Volume of Fluid (VOF) multiphase model. By analyzing the volume fraction field resultant from the simulations, aspects of the bubble shape, such as its nose and the flatness of its rear, the variation of the liquid film height along the bubble and the slug aeration were verified. Mean slug length, translational velocity and frequency were evaluated and showed to be in agreement with literature. Wall shear stresses and momentum flux parameters at the gas and liquid regions were computed. This novel approach may lead to a better estimation of friction factors to be used in one-dimensional models.

5. ACKNOWLEDGEMENTS

The authors thank the Brazilian Government agencies CAPES and CNPq for the continuous support during the development of this research.

6. REFERENCES

Bendiksen, K.H., 1984. “An experimental investigation of the motion of long bubbles in inclined tubes”. *International Journal of Multiphase Flow*, Vol. 10, No. 4, pp. 467–483.

Brackbill, J.U., Kothe, D.B., Zemach, C., 1992. “A Continuum Method For Modeling Surface Tension.” *Journal of Computational Physics*, Vol. 100, N. 2, P. 335-354.

Fernandes, L.S., Martins, F.J.W.A., Azevedo, L.A.A., 2018. “A technique for measuring ensemble-averaged, three-component liquid velocity fields in two-phase, gas–liquid, intermittent pipe flows”. *Experiments in Fluids*, Vol. 59:147.

Lockhart, R.W. and Martinelli, R.C., 1949. “Proposed correlation of data for isothermal two-phase flow, two component flow in pipes”. *Chemical Engineering Progress*, Vol. 45, No. 1, pp. 39–48.

Nieckele, A.O., Carneiro, J.N.E., Chucuya, R.C. and Azevedo, J.H.P., 2013. “Initiation and statistical evolution of horizontal slug flow with a two-fluid model”. *Journal of Fluids Engineering*, Vol. 135.

Menter, F.R., Kuntz, M. and Langtry, R., 2003. “Ten years of industrial experience with the SST turbulence model”. *Turbulence, Heat and Mass Transfer*, Vol. 4, pp. 625–632.

Pineda-Pérez, H., Kim, T., Pereyra, E. and Ratkovich, N., 2018. “CFD modeling of air and highly viscous liquid two-phase slug flow in horizontal pipes”. *Chemical Engineering Research and Design*, Vol. 136, pp. 638–653.

Simões, E.F.; Carneiro, J.N.; Nieckele, A.O., 2014. “Numerical prediction of non-boiling heat transfer in horizontal stratified and slug flow by the Two-Fluid Model”. *International Journal of Heat and Fluid Flow*, Vol.. 47, p.135-145.

Taitel, Y. and Barnea, D., 1990. “Two-phase slug flow”. *Advances in Heat Transfer*, Vol. 20, pp. 83–132.

Thaker,J. and Banerjee, J., 2016. “Influence of intermittent flow sub-patterns on erosion-corrosion in horizontal pipe”, *Journal of Petroleum Science and Engineering*, Vol. 145, pp. 298-320

7. RESPONSIBILITY NOTICE

The authors are the only responsible for the printed material included in this paper.